Sigma Journal of Engineering and Natural Sciences
Web page info: https://sigma.yildiz.edu.tr
DOI: 10.14744/sigma.2022.00066

Research Article

Characterization of friction stir welded AA 3003-H24 aluminum alloy plates

Şefika KASMAN[1]*, Sertan OZAN[2]

[1]*Department of Mechanical Engineering, Dokuz Eylul University, Izmir, Türkiye*
[2]*Department of Mechanical Engineering, Yozgat Bozok University, Yozgat, Türkiye*

ARTICLE INFO

Article history
Received: 08 February 2021
Accepted: 15 June 2021

Keywords:
Friction Stir Welding;
AA 3003 Aluminum Alloy;
Mechanical Properties

ABSTRACT

AA 3003-H24 aluminum alloy plates were butt-welded in order to investigate the effect of friction stir welding process variables on the structural properties of the welded joints. The welded joints were characterized using macro-structural investigations; and tunnel-type defects with varied sizes were detected to occur. At a welding speed of 50 mm/min, tunnel-type defects with large size were found to occur in joints welded with the tool rotational speed of 500 and 1000 rpm. The tunnel-type defects were detected to occur in welded joints produced with the process parameters of 80 mm/min welding speed and 500 and 800 rpm tool rotational speed. However, cavity-type defects were observed to occur at both welding speeds. Even, defects were found to occur in the welded joints, all welded joints were detected to fracture between the base metal and the heat-affected zone, except for the joints welded under the process parameters of 50 mm/min welding speed, 500 and 1000 rpm tool rotational speed. The highest ultimate tensile strength among all the welded joints was measured to be 128 MPa produced under the process parameters of 50 mm/min welding speed and 800 rpm tool rotational speed. It has been revealed that there is a good correlation between the size of the defects and the tensile properties of welded joints. An examination on the fracture surface of the welded joints revealed that welded joints were fractured in ductile manner except the joint produced under the process parameters of 50 mm/min welding speed and 500 rpm tool rotational speed.

Cite this article as: Kasman Ş, Ozan S. Characterization of friction stir welded AA 3003-H24 aluminum alloy plates. Sigma J Eng Nat Sci 2022;40(3):620–629.

INTRODUCTION

The most prominent common point of conventional welding processes is the tendency of production of defected joints. It is accepted to be a critical problem, since the welding process takes place under a liquid phase. At this point, a favorable welding method should be chosen according to material type, thus reducing the probability of formation of

***Corresponding author.**
*E-mail address: sefika.kasman@deu.edu.tr

This paper was recommended for publication in revised form by Regional Editor Amin Shahsavar

defects. Some of aluminum alloys are known to be among the critical material groups in terms of their welding ability using conventional welding techniques due to their high thermal properties, solidification properties, the tendency of the formation oxide layer and hydrogen solubility in the liquid state [1-5]. These features increase the possibility of formation of cavities and cracks in the welded joint, causing welded joints to be fractured in a brittle manner. Taking the defects that occur in the liquid phase into consideration, the advantages of the solid state welding process on the joint strength become prominent. Aluminum alloys are extensively used in industry (e.g. automotive, marine, ship building, chemical equipment and storage tanks) [6-8] due to their inherent properties, e.g. high strength to weight ratio, high resistance to corrosion, heat conductivity and superior workability. The excellent properties that make the aluminum alloys to be most popular materials could get worsen via secondary processes. The welding procedure is accepted to be one of the secondary and complementary process in manufacturing methods. Therefore, it is crucial to choose the proper welding technique in welding process of aluminum alloys. Solid state welding techniques offer many advantages, thus solving the problems [9,10] to be encountered in welded joints.

Friction stir welding (FSW) is one of the solid state welding techniques; joints are produced using specially profiled pins in order to obtain a sound joint. Two different features, namely diameter of shoulder and pin profile, manage the amount of heat input and mixture of materials at the contact area. Friction stir welding is evaluated to be a combination of both hot extrusion and forging processes; the above-mentioned features manage those processes. The frictional heat causes the material to plasticize on the abutted surface of the plates, thereby transferring the plasticized materials along the weld line from the advancing side (AS) of the tool to the retreating side (RS) of the tool pin. In this phenomenon, materials that intimate contact with pin are forged with the stirring effect of pin. Following this process, extrusion starts with the effect of transferring of stirred material into the gap formed by the pin. Those phenomenons occur respectively, constituting the nature of the FSW method. However, above mentioned phenomenons identify the factors that govern the quality of welded joints. Defects, encountered in FSW process, are originated from an improper heat input. Heat input is generated with tool characteristics (namely pin profile, pin and shoulder diameter) and welding parameters (namely tool force, tool rotational speed and welding speed). The defects, seen in FS welded joints, are not encountered in conventional fusion welding processes due to solid phase nature of the welding process. Defects, occurred during fusion welding, are originated from an improper welding process variables, namely improperly selected filler material and unsteady solidification rate of the liquid phase. Some of the aluminum alloys could not be welded using fusion welding techniques due to above-mentioned problems. The invention of the friction stir welding enabled many studies to be performed on aluminum-based alloys; notably, significant improvements have been obtained on the mechanical performance of welded joints. Al-Cu-Mn alloys are one of the alloy groups that could not be welded using fusion welding techniques due to their low process temperature [1, 2]. The AA 3003 is a wrought Al-Fe-Cu-Mn alloy; it is characterized with low strength, high corrosion resistance and superior workability. To the best of our knowledge, there are few studies focusing on the welding ability of AA 3003 alloy using FSW method. Birol et al. [1] studied on AA 3003 aluminum alloy in order to determine the effect of tool rotational speed on weld characteristics using straight threaded tool pin. Another study was performed by Tan et. al. [9]; welded joints were produced using underwater FSW applications to investigate the welding characteristic using a conical screwed pin. Other studies [10-14] were performed to investigate the effect of FSW parameters on mechanical properties and microstructural evolution of FS welded joints. The researchers used cylindrical, conical threaded pin, cylindrical and conical unthreaded pin geometry and investigated the effect of process parameters on microstructural and mechanical evolution of FS welded joints [4,9,11-15]. This study differs from the existing studies in terms of the tool pin profile. In the available literature, no FSW process of AA 3003 alloy has been reported to be using pentagonal pin profile with the assigned values for the selected parameters. It is well known that, to obtain defect-free joints is the main aim of all welding procedures. The pin profile plays a critical role in material flow, exhibiting deterministic effects to obtain defect-free joints associated with the FSW parameters. The effective stirring process is accepted to be crucial criteria in producing defect-free joints. FSW is a process that takes place under the joint effect of both heat and plastic deformation. Notably, when these two variables are in appropriate level, FS welded joints with high mechanical strength and ductility could be produced. Pulsation action aids to increase the plastic deformation intensity during the rotation of tool [16]. The pulses are accepted to be affected from tool rotation speed and number of flat faces. It is worth noting that to increase the number of flat faces results in intense pulsating actions and material flow, thus increasing the intensity of plastic deformation [17]. Pentagonal and hexagonal shaped pins have more flat faces, ensuring them to generate intense pulsating actions in comparison to those of square and triangle shaped pins used [17]. In FSW applications where cylindrical, conical and threaded pin profiles are used, no pulsating action has been reported to exist [16]. Eccentricity is a variable which is well-known to exhibit an effect in producing defect-free welded joints; notably it is activated when using polygonal profiled pins. The eccentricity

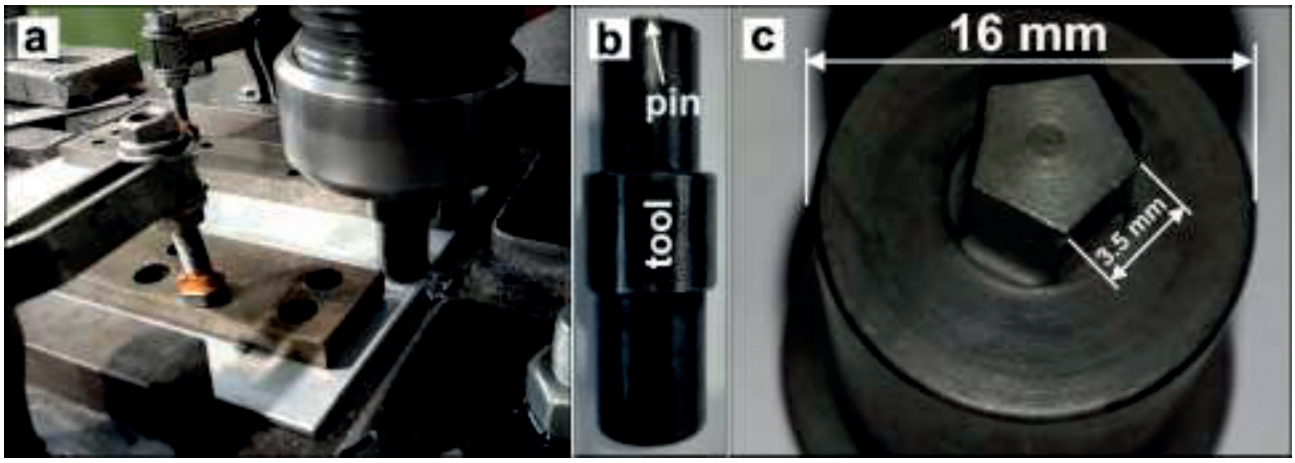

Figure 1. FSW process (a) position of plates; (b) tool pin profile; (c) top view of pin profile and dimension.

Table 1. The chemical composition of AA 3003 (wt. %)

Alloy / Elements	Mn	Fe	Si	Cu	Mg	Zn	Ti	Al
AA 3003– H24	1.051	0.384	0.116	0.052	0.006	0.01	0.023	Bal.

phenomenon enables incompressible material to move around the pin profile [17].

The number of flat surfaces of a polygonal pin determines the intensity of frictional heat generation produced during the FSW process. In the study of Patel et. al. [18], at the end of the plunge stage, pentagonal pin profile resulted in obtaining maximum temperature of 373˚C, exhibiting higher temperature value than those of hexagonal, square and conical pin profiles. Pentagonal shaped pin was reported to produce maximum temperature [18]. Polygonal pins were reported to exhibit closeness to the linearity curve of maximum temperature values during the plunge stage, thereby revealing the uniform rise of temperature at the increased plunge depth [18]. Pentagon pin profile was reported to exhibit the best linearity curve, meaning that uniform temperature rise at all the plunge depth [18].

The present study differs from the other studies in the context of pin geometry. The pentagonal profiled pin was used to form a weld bond between the AA 3003-H24 aluminum alloy plates. AA 3003-H24 aluminum alloy was work hardened and then partially annealed. The main aim of this study is to investigate the effect of FSW process parameters and pentagonal profiled pin on the mechanical properties and microstructural evolution of FS welded joints.

EXPERIMENTAL PROCEDURES

The chemical composition of AA 3003-H24 plates, which is the subject of the present study, is given in Table 1. The plates with a thickness of 3 mm were machined into 100 mm width and 225 mm length. The plates were placed on a backing plate in order to provide a tight contact between plates, thus eliminating the separation of the plates during welding process as shown in Fig. 1. The FSW processes were performed on the universal milling machine using a pentagonal shaped a pin made of H13 tool steel. The hardness value of tool was 50-52 HRC. The pin configurations, position of plates and details of plate support are shown in Fig. 1. The tool was rotated clockwise with 2 degrees of tilting angle for 10 seconds before moving across the contact surface of the plates. In order to perform FSW process, three different tool rotational speeds of 500, 800 and 1000 rpm and two different welding speeds of 50 and 80 mm/min were selected as process parameters.

Table2. Arrangement of experiments for use in FSW applications

Welded Joints	Process Parameters	
	TRS	WS
W1	500	50
W2	800	50
W3	1000	50
W4	500	80
W5	800	80
W6	1000	80

Microstructural observations were performed following the standard metallographic procedures applied on the cross-sectional surface of the weld line. Specimens were etched using Keller solution. The etching time was 60 s. The mechanical properties of welded joints were characterized by tensile properties (ultimate tensile strength and elongation at rupture) and micro-hardness. Three different tensile test specimens of each FSW combination were prepared. The specimens were cut perpendicular to the weld line; they were tested with a cross-head speed of 2 mm/min at room temperature. The gauge length was determined to be 50 mm. The micro-hardness test of each FSW specimens was performed on the cross-section of welded joint consisting of weld regions, namely stir zone (SZ), thermo-mechanically affected zone (TMAZ) and heat affected zone (HAZ). The micro-hardness measurements were carried out on the center of weld thickness with 1.5 mm intervals using a load of 100 g for 15 s.

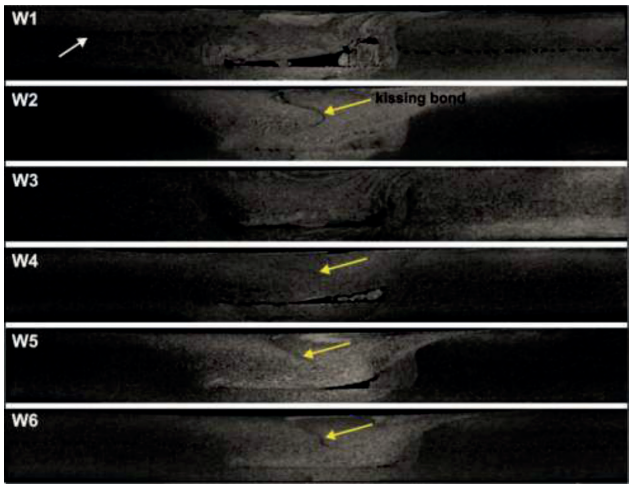

Figure 2. Macrostructure of FS welded specimens.

RESULTS AND DISCUSSION

Macrostructural and Microstructural investigation of joints

The macrostructure of the welded joints is seen in Fig. 2. The detailed observations on the weld area revealed that defects with different sizes were located in the SZ close to the advancing side (AS) of root of weld line. Macro-sized tunnel-type defects were detected in the SZ of W1, W3, W4 and W5 welded joints. It was revealed that defects started from RS and grew towards to AS, indicating that improper and insufficient material flow was involved. When the size and shape of defects were investigated, it was observed that those types of defects were the tunnel-type defects. The occurrence of tunnel-type defect was reported to be originated from lack of material flow between plates due to inadequate heat generation and/or improper material flow [11,15,16,19-21]. The FSW technique is a combination of both extrusion and forging processes. The inadequate heat generation causes plastic deformation not to occur properly. A sufficient material flow is evaluated to be possible in case appropriate heat conditions are provided. A weld seam in FSW occurs by the following way; the pin rotates and moves along the weld line, filling the carried material into the gap left behind. It is actually evaluated to be a kind of extrusion process. In case the generated heat is insufficient, the extrusion process occurs improperly. Therefore, the tunnel-type defects, seen in the joints (see Fig. 2), were originated from an improper extrusion process. The AA 3003 aluminum alloy contains Mn, Fe and Si elements and α-Al_{12}(Mn,Fe)3Si intermetallic particles as reported elsewhere [1,22,23]. XRD analysis was performed on base metal, W3 and W5 welded joints. XRD patterns belonging to base metal, SZ of W3 and W5 welded joints are given in Fig. 3. Al(Mn,Fe)Si and Al_6(Mn,Fe) phases were detected to occur via XRD analysis. Similar findings were reported elsewhere [9,24]. It is worth noting that base metal, W3 and W5 welded joints exhibited similar phases.

Figs. 4 and 5 exhibit the cross-section of welded joint consisting of three characteristic zone, namely HAZ, TMAZ and SZ [16]. As can be seen in Fig. 4 and Figs. 5b-c, the size of intermetallic particles detected in the base metal was coarser than the particles detected in SZ. These intermetallic particles were clustered and oriented towards to the direction of tool rotation in the SZ. A structural feature was observed in all the welded joints. A representative feature, namely kissing bond is shown in Fig. 5d. Even, those features are evaluated to be a defect [19,21,25], the effects of kissing bond formations on the mechanical properties are not significant. There are two opinions which were put forward regarding the kissing bond; one of them is the kissing bond formation with the broken oxides on the adjacent surface of the plates to be joined [19,26,27]. The oxide layers are evaluated to be broken with the effect of tool pressure. Those broken oxide particles find a way via tool rotation direction, completing their movement under the shoulder of the tool in the S curve. Kissing bonds exhibit a S-type curve. The discontinuity of a weld bond is attributed to the presence of oxide layers. The other opinion is that kissing bond formations are originated from insufficient pressure and inadequate mixing effect of the material in the contact line of plates [19]. According to those two opinions, existence of the kissing bond in SZ creates a discontinuity in the welded joint. In this study, the effect of kissing bond on the mechanical properties was not evident due to tunnel-type defects in SZ.

A typical weld zone in FS welded joints consists of three characteristic zones as seen in Fig. 4. The SZ is under the effect of two features, namely intense plastic deformation and heat input. Those properties cause the deformed

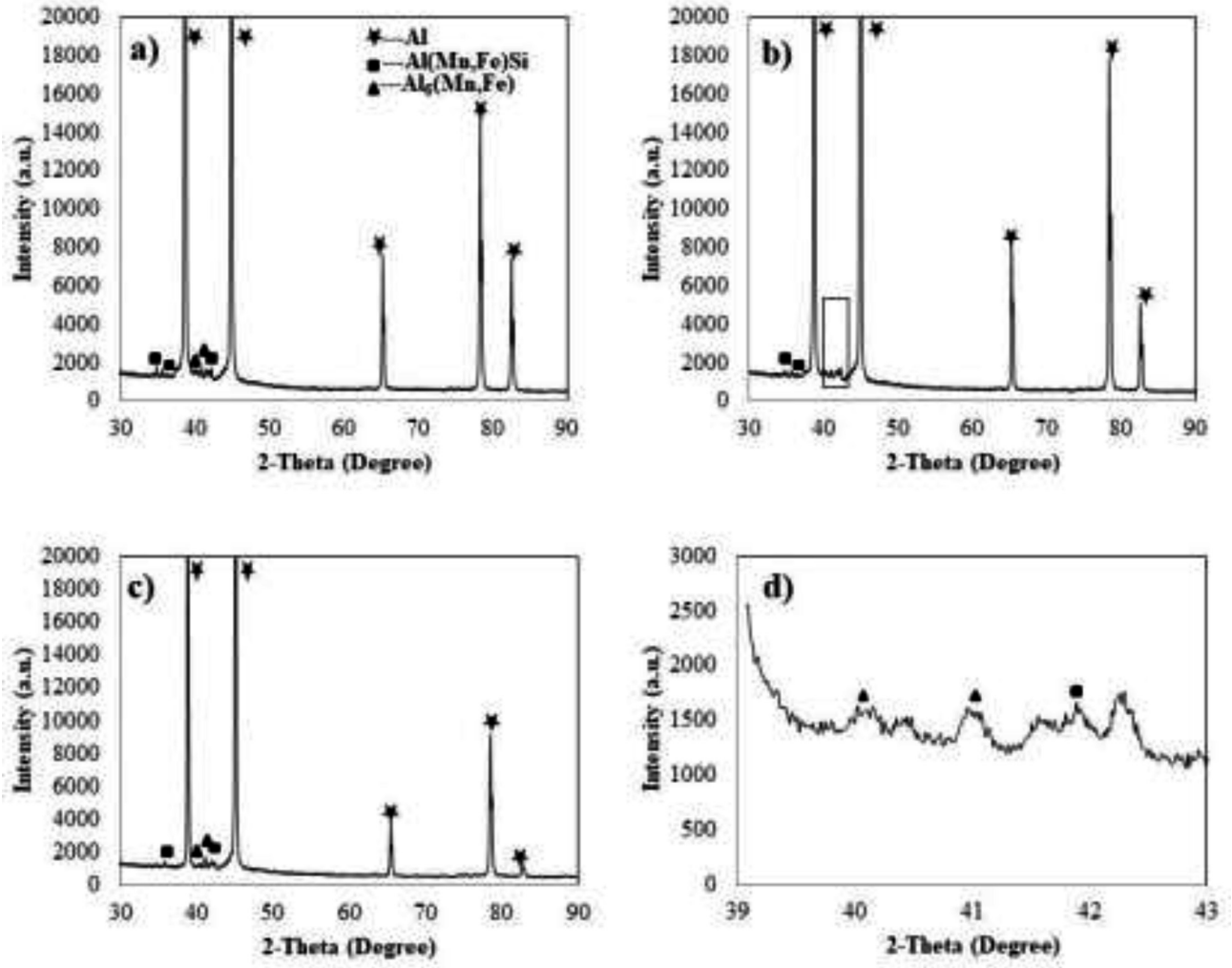

Figure 3. XRD patterns of specimens (a) W3-SZ; (b); W5-SZ; (c) base metal; (d) magnified peaks marked by a rectangular in (b).

Figure 4. The transition zones for W2 welded joint.

coarse-sized grains to shrink via activating the recrystallization mechanism. A clear observation in the zones seen in Figs. 4 and 5 revealed that the changes in the grain size of the regions stand out. While relatively finer grains were found to occur in the SZ, the coarser and deformed grains along the tool rotation direction were observed to occur in HAZ and TMAZ. It has been found that thermal effects of friction between tool and metals led to a change in grain size.

Welded joints' mechanical properties and characteristics

Stress-strain curves of welded joints and base metals are given in Fig. 6. The average of three UTS and ε_p (%) values were used to evaluate the relationship between welding parameters and tensile properties. Tensile properties of welded joints and base metal are given in Table 3. The inference from the tensile test results is that TRS and

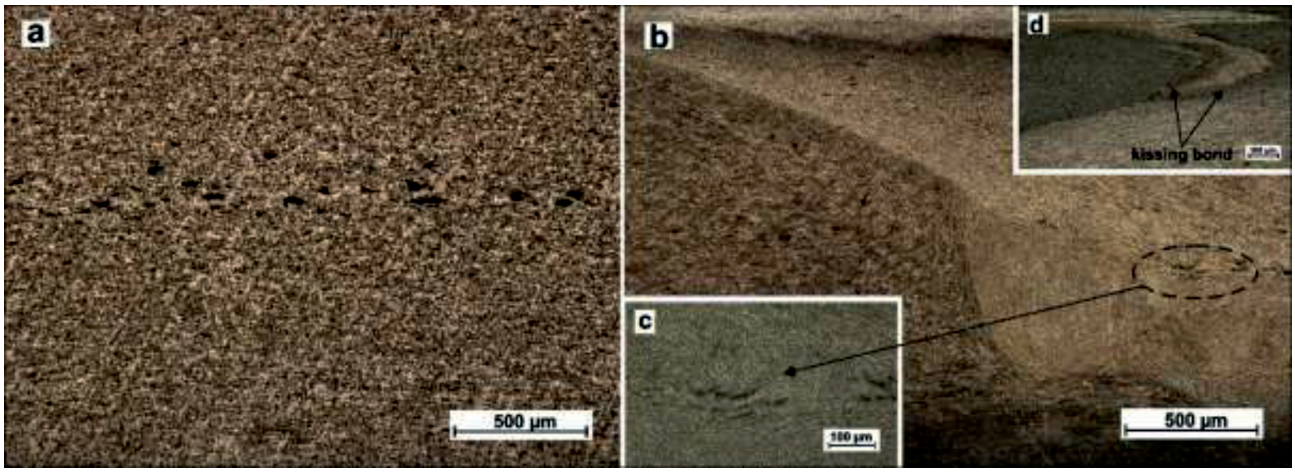

Figure 5. The segments in both base metal (a) and SZ of W5 (b and c), kissing bond in the SZ of W5 (d).

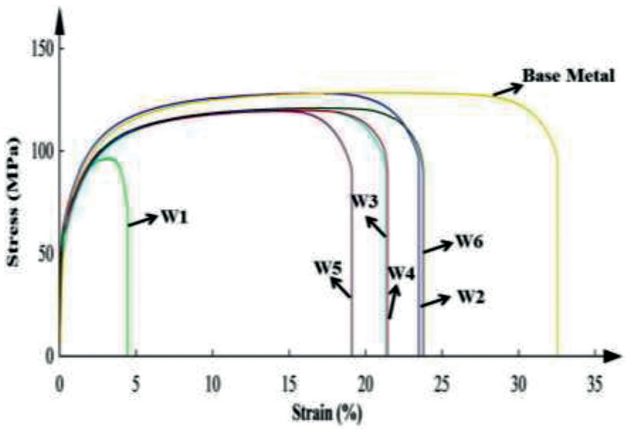

Figure 6. Stress-strain curves of welded joints and base metal.

Table 3. Tensile properties of welded joints and base metal

Welded Joints	Tensile Strength (MPa)	Elongation at Rupture (%)
Base Metal	129 ± 1	31 ± 2
W1	91 ± 9	5 ± 1
W2	128 ± 0	23 ± 3
W3	119 ± 1	19 ± 4
W4	120 ± 0	18 ± 4
W5	119 ± 1	18 ± 3
W6	121 ± 1	24 ± 1

WS were found to be effective on the tensile properties of joints.

The fracture location of welded joints after tensile test is given in Fig. 7. The fracture location of each welded joints except W1 and W3 welded joints was found to locate on the outside region of the weld seam. The lowest UTS was obtained under the process parameters of 500 rpm TRS and 50 mm/min WS. It is obvious that UTS value of 91 ± 9 MPa is attributed to a large volumetric tunnel-type defect in SZ. The tunnel-type defects led to a decrease in the tensile properties. A larger tunnel-type defect resulted in a decrease of elongation at rupture of W1 welded joint. The tunnel-type defect in W1, seen in Fig. 2, caused the weld seam to break in SZ as seen in Figs. 7a and 7b. The elongation at rupture of W1 was measured to be 5 ± 1 (%), indicating the brittle manner of W1 welded joint. W2 welded joint exhibited the highest UTS value of 128 MPa; notably, W2 welded joint was produced with the process parameters of 800 rpm TRS and 50 mm/min WS. The weld seam was detected to be broken on base metal side as seen in Figs. 7a and 7b, therefore meaning that a strong weld seam was formed between the two plates. However, cavity-type defects were found to occur in W2 welded joint as seen in Fig. 2. Although W2 welded joint was detected to contain defects, neither the UTS nor the ε_p (%) values was affected by this defect. When an observation was performed in Fig. 2, it would be seen that all welded seams contain defects with varied sizes. The welded joints, W2 and W6, were observed to contain cavity-type defects with finer sizes. However, the process parameters were different from each other, thus meaning that both TRS and WS were effective on the UTS value. The most influential factor on weld quality was evaluated to be the presence of a defect.

The fracture surface of FS welded joints was observed using a scanning electron microscope (SEM). The fracture surfaces, examined following the tensile test are shown in Fig. 8. When the fracture surface of the W2, 3, 4, 5 and 6 FS

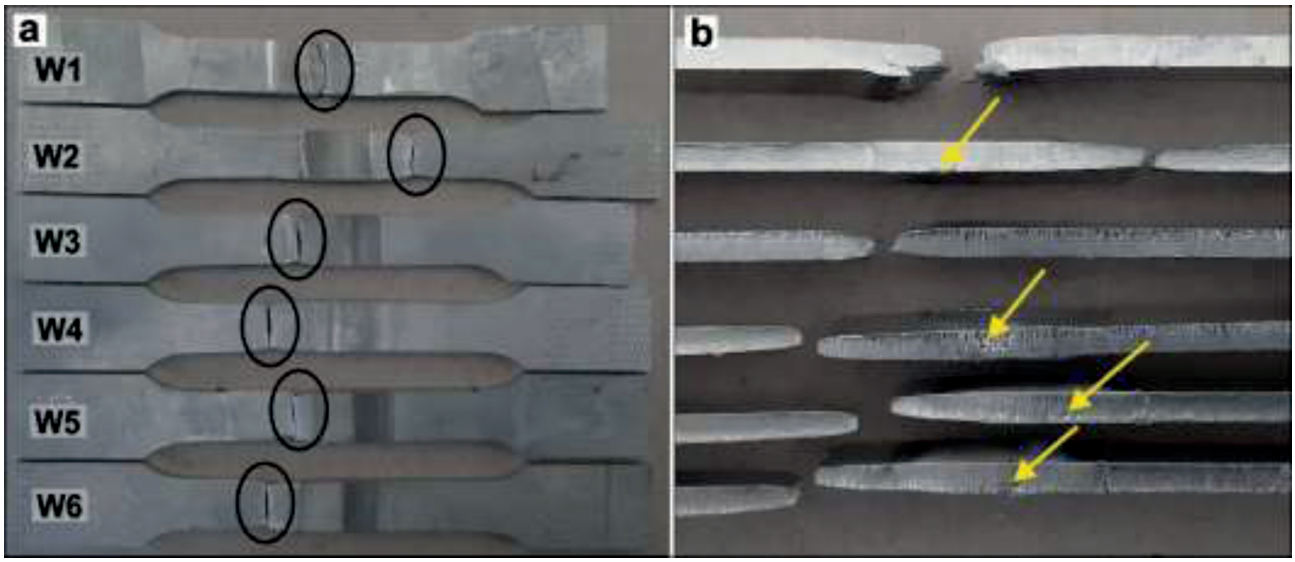

Figure 7. The fracture location of FS welded joints.

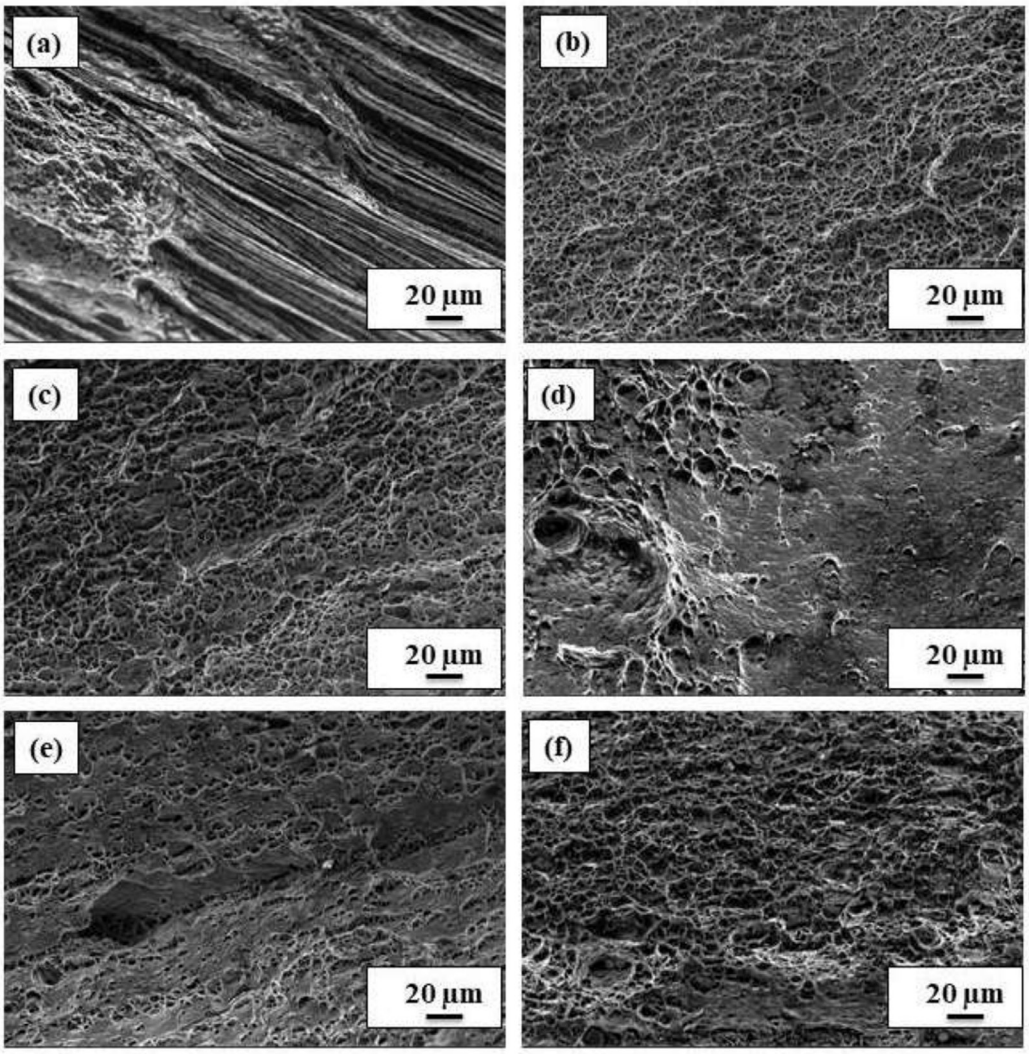

Figure 8. Fracture surface of welded joints (a) W1; (b) W2; (c) W3; (d) W4; (e) W5; (f) W6.

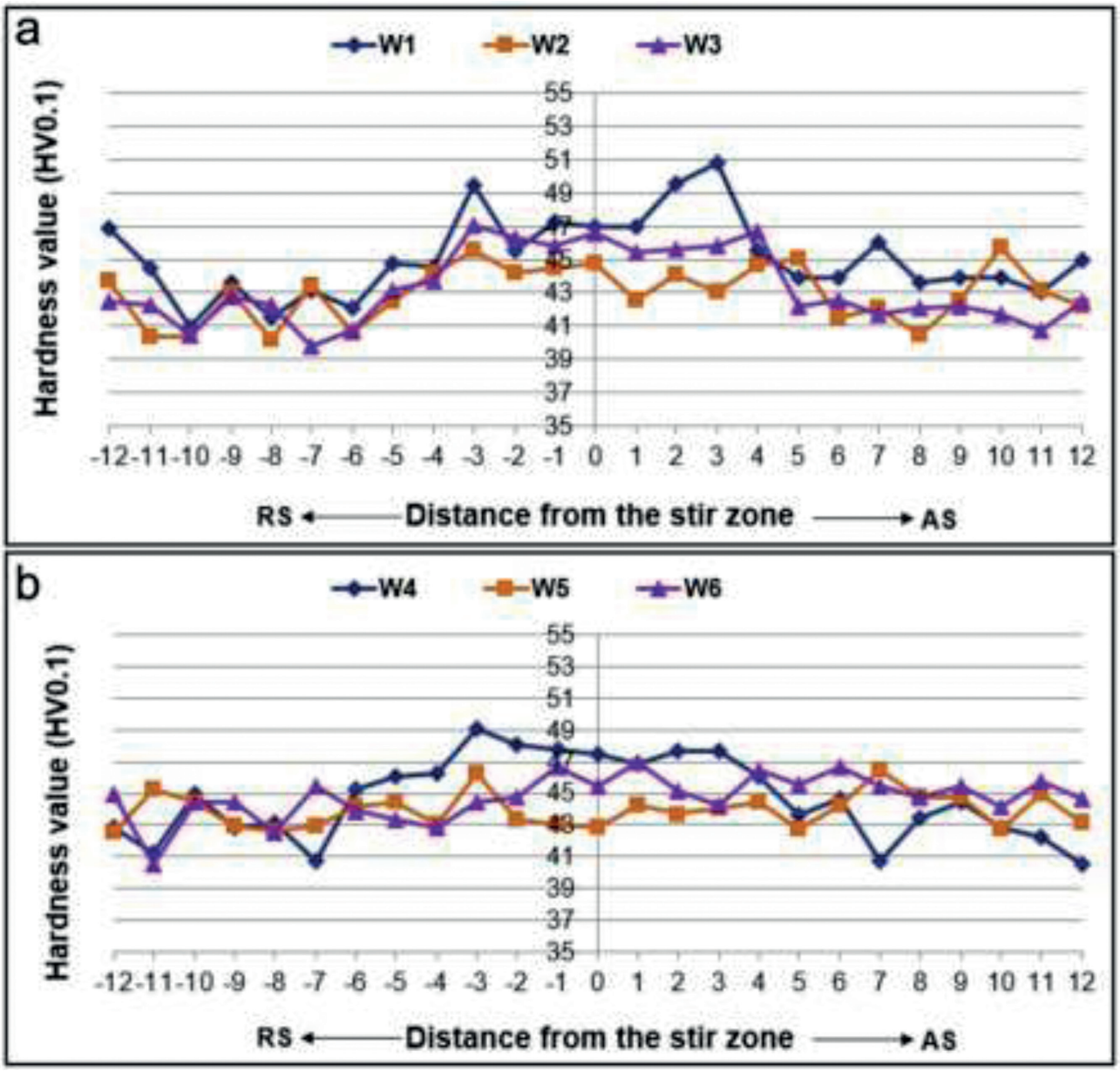

Figure 9. The fluctuating hardness profile that runs through the weld zone.

welded joints was examined, it was observed that the fracture surfaces were consisted of dimple formations. It was revealed that no significant amount of plastic deformation occurred in W1 welded joint, revealing that it was fractured in a brittle manner. Notably, W1 joint exhibited the lowest ductility among FS welded joints. Fracture surface of W1 joint was found to be flatter.

Micro-hardness profiles

The micro-hardness test results are given in Fig. 9. Taking the change of WS into consideration, the welded joints were divided into two groups. The micro-hardness values in the SZ of the W1 welded joint, produced with 50 mm/min WS, were relatively higher than those of in HAZ and BM. The highest micro-hardness values were achieved in the SZ which is located near TMAZ. When the change in the maximum and minimum hardness values was investigated, the change in micro-hardness of W1-SZ, produced with WS of 50 mm/min, was more pronounced than the other two welded joints (W2 and W3). The micro-hardness distribution of W1-W3 welded joints exhibited a similar trend, tracking a W-shaped profile. The hardness distribution of W4-W6 welded joints along the SZ was measured to be uniform and the change in hardness value was evaluated to be negligible as reported elsewhere [28]. As mentioned in the study of Birol et.al. [1], in case the dynamic

recrystallization does not occur properly, the hardness of SZ is higher than that of base metal due to intense plastic deformation. The distributions of micro-hardness values of the first group welded joints were similar to those of micro-hardness values of the second group. The highest micro-hardness values in SZ of each group were obtained when the welded joints were produced with 500 rpm TRS. Those welded joints were detected to contain a large tunnel-type defect. A tunnel-type defect occurs under conditions where there is improper material flow in SZ due to insufficient heat input. Insufficient heat input is evaluated to be the reason of cold working conditions. The highest micro-hardness values in welded joints, produced with the process parameter of 500 rpm TRS, were attributed to the cold working conditions.

CONCLUSIONS

The present study was carried out to reveal the effects of TRS and WS on the mechanical properties of welded joints manufactured using pentagonal shaped tool pin. The joints, welded with a TRS of 500 rpm were observed to contain macro-sized tunnel-type defect. While this defect exhibited its negative effect on the UTS of the welded joint produced with the process parameter of 50 mm/min WS via breaking in the SZ, this was not the case for 80 mm/min WS. The UTS and ε_p (%) of this specimen were measured to be 91 ± 9 MPa and 5 ± 1 (%), respectively. This joint exhibited the worst mechanical properties among all welded joints. The UTS and ε_p (%) of welded joints were improved significantly with increasing TRS and WS. Among all welded joints, the highest joint strength was measured to be 128 MPa; this joint was produced with the process parameters of 800 rpm TRS and 50 mm/min WS. The UTS of this welded joint was compared with the UTS of the base plate (129 MPa), finding that there was no significant difference between the UTS of base metal and W2 welded joint. Tensile test results revealed that although SZ exhibited defects, the welded joints apart from the W1 and W3 welded joints were fractured outside the weld zone, exhibiting a perfect correlation between tensile properties and size of defects detected in SZ. The intermetallic particles in the base metal were observed in weld zones, namely SZ and TMAZ; they were found to be dispersed along the tool rotation direction. The kissing bond was found to occur in the SZ; however it did not affect the mechanical performance of the welded joints. Notably, different types of polygonal shaped pins could be used in FSW process of AA 3003 alloy in order to reveal their effect on mechanical performance of FS welded joints.

ACKNOWLEDGEMENT

The present study was supported by Dokuz Eylul University under project no. 2017.KB.FEN.002. The authors would like to acknowledge this financial support.

AUTHORSHIP CONTRIBUTIONS

Authors equally contributed to this work.

DATA AVAILABILITY STATEMENT

The authors confirm that the data that supports the findings of this study are available within the article. Raw data that support the finding of this study are available from the corresponding author, upon reasonable request.

CONFLICT OF INTEREST

The author declared no potential conflicts of interest with respect to the research, authorship, and/or publication of this article.

ETHICS

There are no ethical issues with the publication of this manuscript.

REFERENCES

[1] Birol Y, Kasman S. Friction stir welding of twin-roll cast EN AW 3003 plates. Met Mater-Int 2013;19:1259–1266.

[2] Genevois C, Deschamps A, Denquin A, Doisneau-cottignies B. Quantitative investigation of precipitation and mechanical behaviour for AA2024 friction stir welds. Acta Mater 2005;53:2447–2458. [CrossRef]

[3] Dialami N, Chiumenti M, Cervera M, de Saracibar CA. An apropos kinematic framework for the numerical modeling of friction stir welding. Comput Struct 2013;117:48–57. [CrossRef]

[4] Bozkurt Y, Duman S. The effect of welding parameters on the mechanical and microstructural properties of friction stir welded dissimilar AA 3003-H24 and 2124/SiC/25p-T4 alloy joints. Sci Res Essays 2011;6:3702–3716. [CrossRef]

[5] Heidarzadeh A, Mironov S, Kaibyshev R, Cam G, Simar A, Gerlich A, et al. Friction stir welding/processing of metals and alloys: A comprehensive review on microstructural evolution. Prog Mater Sci 2021;117:68. [CrossRef]

[6] Boulahem K, Ben Salem S, Bessrour J. Prediction model of ultimate tensile strength and investigation on microstructural characterization of friction stir welded AA2024-T3. Int J Adv Manuf Technol 2018;95:1473–1486. [CrossRef]

[7] Meng XC, Huang YX, Cao J, Shen JJ, dos Santos JF. Recent progress on control strategies for inherent issues in friction stir welding. Prog Mater Sci 2021;115:74. [CrossRef]

[8] Dialami N, Cervera M, Chiumenti M. Defect formation and material flow in Friction Stir Welding. Eur J Mech A-Solids 2020;80:13. [CrossRef]
[9] Tan YB, Wang XM, Ma M, Zhang JX, Liu WC, Fu RD, et al. A study on microstructure and mechanical properties of AA 3003 aluminum alloy joints by underwater friction stir welding. Mater Charact 2017;127:41–52. [CrossRef]
[10] Abnar B, Kazeminezhad M, Kokabi AH. Effects of heat input in friction stir welding on microstructure and mechanical properties of AA3003-H18 plates. Trans Nonferrous Met Soc China 2015;25:2147–2155. [CrossRef]
[11] Dehghani M, Mousavi S, Amadeh A. Effects of welding parameters and tool geometry on properties of 3003-H18 aluminum alloy to mild steel friction stir weld. Trans Nonferrous Met Soc China 2013;23:1957–1965. [CrossRef]
[12] Aydin H, Bayram A, Yildirim MT, Yigit K. Influence of Welding Parameters on the Fatigue Behaviours of Friction Stir Welds of 3003-O Aluminum Alloys. Mater Sci-Medzg 2010;16:311–319. [CrossRef]
[13] Abdulrehman MA, Challoob SH, Marhoon II. Investigation of mechanical and numerical properties of friction stir welding (FSW) for 3003 - H14 Aluminum Alloys. Defect and Diffusion Forum 2020;398:106–116. [CrossRef]
[14] Aydın H, Tutar M, Yiğit K, Bayram A. Mechanical properties of friction stir welded 3003 aluminum alloy in different welding conditions. Int J Mech Prod Eng 2017;5:92–96.
[15] Palanivel R, Mathews PK, Murugan N, Dinaharan I. Effect of tool rotational speed and pin profile on microstructure and tensile strength of dissimilar friction stir welded AA5083-H111 and AA6351-T6 aluminum alloys. Mater Des 2012;40:7–16. [CrossRef]
[16] Elangovan K, Balasubramanian V. Influences of tool pin profile and welding speed on the formation of friction stir processing zone in AA2219 aluminium alloy. J Mater Process Technol 2008;200:163–175. [CrossRef]
[17] Patel VV, Badheka V, Kumar A. Friction stir processing as a novel technique to achieve superplasticity in aluminum alloys: process variables, variants, and applications. Metallogr Microstruct Anal 2016;5:278–293. [CrossRef]
[18] Patel VV, Badheka VJ, Kumar A. Influence of pin profile on the tool plunge stage in friction stir processing of Al-Zn-Mg-Cu Alloy. Trans Indian Inst Met 2017;70:1151–1158. [CrossRef]
[19] Khan NZ, Siddiquee AN, Khan ZA, Shihab SK. Investigations on tunneling and kissing bond defects in FSW joints for dissimilar aluminum alloys. J Alloy Compd 2015;648:360–367. [CrossRef]
[20] Elangovan K, Balasubramanian V, Valliappan M. Effect of tool pin profile and tool rotational speed on mechanical properties of Friction Stir Welded AA6061 aluminium alloy. Mater Manuf Process 2008;23:251–260. [CrossRef]
[21] Elangovan K, Balasubramanian V, Babu S. Developing an empirical relationship to predict tensile strength of friction stir Welded AA2219 Aluminum Alloy. J Mater Eng Perform 2008;17:820–830. [CrossRef]
[22] Birol Y, Kasman S. Effect of welding parameters on the microstructure and strength of friction stir weld joints in twin roll cast EN AW Al-Mn1Cu plates. J Mater Eng Perform 2013;22:3024–3033. [CrossRef]
[23] Huang HW, Ou BL. Evolution of precipitation during different homogenization treatments in a 3003 aluminum alloy. Mater Des 2009;30:2685–2692. [CrossRef]
[24] Long L, Pan QL, Li MJ, Ye J, Sun YQ, Wang WY, et al. Study on microstructure and mechanical properties of 3003 alloys with scandium and copper addition. Vacuum 2020;173:109112. [CrossRef]
[25] Sato YS, Takauchi H, Park SHC, Kokawa H. Characteristics of the kissing-bond in friction stir welded Al alloy 1050. Mater Sci Eng A-Struct Mater Prop Microstruct Process 2005;405:333–338. [CrossRef]
[26] Cabibbo M, Forcellese A, Santecchia E, Paoletti C, Spigarelli S, Simoncini M. New approaches to friction stir welding of aluminum light-alloys. Metals 2020;10:233. [CrossRef]
[27] Anand R, Sridhar VG. Studies on process parameters and tool geometry selecting aspects of friction stir welding - A review. Mater Today-Proc 2020;27:576–583. [CrossRef]
[28] Dong JH, Gao C, Lu Y, Han J, Jiao XD, Zhu ZX. Microstructural characteristics and mechanical properties of bobbin-tool friction stir welded 2024-T3 aluminum alloy. Int J Miner Metall Mater 2017;24:171–178. [CrossRef]